HYBRID FUZZY PROPORTIONAL PLUS INTEGRATOR CONVENTIONAL CONTROLLER OF A NOVEL BDFIG FOR WIND ENERGY CONVERSION SYSTEMS

Zoheir TIR*, Rachid ABDESSEMED**
* LEVRES - Research Laboratory, Department of Electrical Engineering, Faculty of Technologies and science, University of Eloued, B.P.789, 39000, El-Oued, Algeria, e-mail: tir-zoheir@univ-eloued.dz
** LEB – Research Laboratory, Department of Electrical Engineering, Faculty of Technologies and science, University of Batna, 05000 Batna, Algeria, e-mail: r.abdessemed@lycos.com

ABSTRACT

This paper discusses the control of a new topology of a brushless doubly-fed induction generator (BDFIG) using back-to-back PWM converters and its application to variable speed wind energy generation. The BDFIG has gained renewed attention in variable speed drive applications in recent years for the features of simple structure, favorable characteristics and economical operation. The goal of BDFIG control is to achieve a similar dynamic performance to the doubly fed induction generator (DFIG), exploiting the well-known induction motor vector control philosophy. The performance of hybrid fuzzy proportional plus integrator conventional (HFP+IC) controller has been investigated and compared with the conventional PI controller based BDFIG. The simulation results show that HFP+IC controller is superior to PI controller under dynamic condition.

Keywords: *Brushless doubly fed induction generator, hybrid fuzzy proportional plus integrator conventional (HFP+IC), PI controller, back-to-back PWM converters, power flow, wind energy system*

1. INTRODUCTION

Currently to the industry is heavily relying on the doubly fed induction generators (DFIG) for variable speed wind energy applications [1, 3] and [4]. The use of the DFIG, however, increased the cost and complexity of the wind turbines [1, 5, 6, and 7] and [11]. The problems were caused by the configuration of the DFIG, which required a wound-type rotor and commutation brushes for the power transfer to or from the rotor windings [5-7] and [11]. These aspects created the need for frequent inspections and maintenance.

To overcome these disadvantages, a solution consists in using a brushless doubly fed induction generator (BDFIG) as shown in Fig. 1. The BDFIG is composed of two three-phase windings in the stator [called power winding (PW) and control winding (CW)] and a special rotor winding is presented in Fig. 2 [3,4,6,8-11].

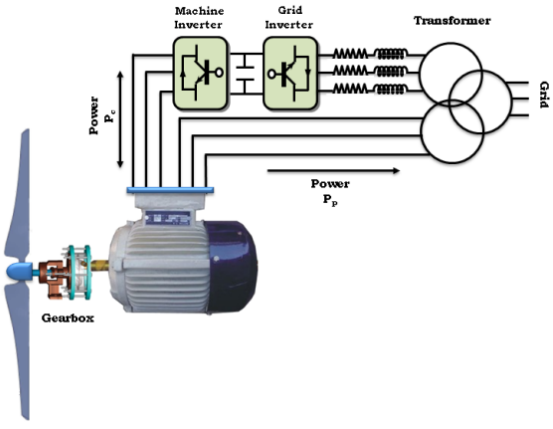

Fig. 1 BDFIG Configuration for Wind Power Generation

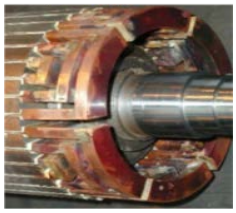

Fig. 2 Photograph of the rotor winding of the BDFIG, [10,12]

However, it allows putting a converter between the CW and the grid which is designed only for a part of the full power of the machine (about 30 %) [4, 6, 8-11]. By controlling correctly this converter, variable-speed operation is allowed and electrical power can be produced from the PW to the grid and also from the CW to the grid.

This paper presents a hybrid fuzzy proportional plus integrator conventional (HFP+IC) controller is proposed for a BDFIG. This HFP+IC controller is constructed by using a fuzzy logic controller in place of the proportional term in the conventional PI controller. The HFP+IC controller combines the advantages of a fuzzy logic controller and a conventional controller.

The fuzzy proportional (FP) term plays an important role in improving overshoot and rise time response [13]. The conventional integral term reduces a steady-state error [13].

Furthermore, this controller has the following features, [13].

1) Since it has only one additional parameter to be adjusted based on the original PI controller it is easy to design.

2) The HFP+IC controller keeps the simple structure of the PI controller. It is not necessary to modify any hardware parts of the original control system for implementation.

3) The sufficient stability condition shows that the same stability remains unchanged if the original PI controller is replaced by the HFP+IC controller.

In this paper the application of HFP+IC for controlling the active and reactive powers of BDFIG is investigated. The performance of HFP+IC controller has been investigated and compared with the conventional PI controller based machine.

Depending on the values of the average (steady state) wind speed, four zones may be identified in the static operation of BDFIG. Zones I and VI, where the provided power is zero, are not concerned by this paper. The interest is here focused on zone II, called partial load zone, where the extracted power proportionally depends of the wind speed cubed, and the so call load zone (III), where the power must be limited to the nominal value.

2. MODELLING OF THE WIND TURBINE AND GEARBOX

The theoretical power available in the wind is defined by Betz formula. It is given by

$$P_w = \frac{1}{2} \cdot \rho \cdot S \cdot v_w^3 \tag{1}$$

Where ρ is the air density (ρ = 1.225 kg/m3) , S is the cross-sectional area of the turbine rotor and v_w is the wind speed.

The effective efficiency conversion is given by the power coefficient (C_p), which is expressed by the following:

$$C_p = \frac{P_t}{P_w} \tag{2}$$

Where P_t is the mechanical power of the turbine and P_w is the available wind power.

The (per unit) speed or relative λ is the ratio between the linear blade speed and the speed of the wind.

$$\lambda = \frac{\Omega_t R}{v_w} \tag{3}$$

Where Ω_t is the turbine speed and R is the turbine radius.

A typical relationship between C_p and λ is shown in Fig. 3. It is clear from this figure that there is a value of λ for which C_p is maximum and that maximize the power for a given wind speed. The peak power for each wind speed occurs at the point where C_p is maximized. To maximize the generated power, it is therefore desirable for the generator to have a power characteristic that will follow the maximum C_{p_max} line.

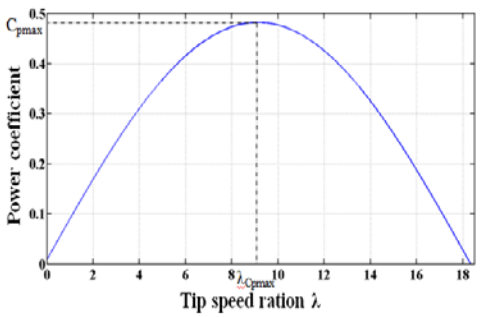

Fig. 3 The Power coefficient for the wind turbine model

Taking into account equations (1), (2) and (3), power on the out axle of the turbine is then:

$$P_t = \frac{1}{2}.C_p.\rho.\pi.R^5.\frac{\Omega_t}{\lambda^3} \tag{4}$$

Torque is then:

$$C_t = \frac{P_t}{\Omega_t} \tag{5}$$

$$C_{em} = \frac{P_t}{\Omega_t} = \frac{1}{2} \cdot \rho \cdot \pi \cdot R^3 \cdot C_p \cdot v_w^3 \tag{6}$$

With the multiplier of report/ratio G, the torque and speed become at shaft end;

$$C_g = \frac{C_t}{G} \text{ and } \Omega_t = \frac{\Omega_{mec}}{G} \tag{7}$$

When the turbine is coupled to a machine the mechanical equation at shaft end will be:

$$J\frac{d\Omega_{mec}}{dt} + f\Omega_{mec} = C_g - C_{em} \tag{8}$$

From these various equations the mathematical model of the turbine at shaft end is shown on Fig. 4.

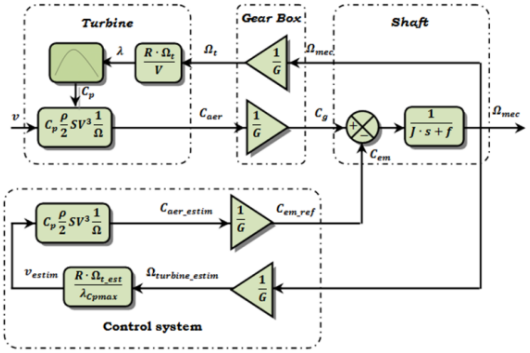

Fig. 4 Device control without control speed, [13]

The expression of the optimal mechanical power P_{mec_opt} is obtained as follows:

$$P_{mec_{opt}} = \frac{1}{2}\frac{C_{p_{max}} \cdot \rho \cdot \pi \cdot R^3}{G^3 \lambda_{opt}^3} \cdot \Omega_{mec}^3 \tag{9}$$

3. DYNAMICAL MODEL OF THE BDFIG

The electrical equations of the BDFIG in the synchronous reference frame (d-q) are this given by [3], [4], [6], [9]:

$$v_{sp}^q = R_{sp} i_{sp}^q + \frac{d\psi_{sp}^q}{dt} + \omega_p \psi_{sp}^d \tag{10}$$

$$v_{sp}^d = R_{sp} i_{sp}^d + \frac{d\psi_{sp}^d}{dt} - \omega_p \psi_{sp}^q \tag{11}$$

$$0 = R_r i_r^q + \frac{d\psi_r^q}{dt} - (\omega_p - p_p \omega_r)\psi_r^d \tag{12}$$

$$0 = R_r i_r^d + \frac{d\psi_r^d}{dt} - (\omega_p - p_p \omega_r)\psi_r^q \tag{13}$$

$$v_{sc}^q = R_{sc} i_{sc}^q + \frac{d\psi_{sc}^q}{dt} + (\omega_p - (p_p + p_c)\omega_r)\psi_{sc}^d \tag{14}$$

$$v_{sc}^d = R_{sc} i_{sc}^d + \frac{d\psi_{sc}^d}{dt} + (\omega_p - (p_p + p_c)\omega_r)\psi_{sc}^q \tag{15}$$

The expressions for stator and rotor flux linkages are

$$\psi_{sp}^{q} = L_{sp} i_{sp}^{q} + L_{mp} i_{r}^{q} \quad (16)$$

$$\psi_{sp}^{d} = L_{sp} i_{sp}^{d} + L_{mp} i_{r}^{d} \quad (17)$$

$$\psi_{r}^{q} = L_{mp} i_{sp}^{q} + L_{r} i_{r}^{q} + L_{mc} i_{sc}^{q} \quad (18)$$

$$\psi_{r}^{d} = L_{mp} i_{sp}^{d} + L_{r} i_{r}^{d} + L_{mc} i_{sc}^{d} \quad (19)$$

$$\psi_{sc}^{q} = L_{sc} i_{sc}^{q} + L_{mc} i_{r}^{q} \quad (20)$$

$$\psi_{sc}^{d} = L_{sc} i_{sc}^{d} + L_{mc} i_{r}^{d} \quad (21)$$

where $i_{sp}^{q}, i_{sp}^{d}, i_{sc}^{q}$ and i_{sc}^{d} are d, q-axis stator currents respectively; i_{r}^{q} and i_{r}^{d} are d, q-axis rotor currents respectively; $\psi_{sp}^{q}, \psi_{sp}^{d}, \psi_{sc}^{q}$ and ψ_{sc}^{d} are d, q-axis stators flux respectively; R_{sp}, R_{sc} and R_r are the stators and rotor resistances per phase respectively; L_{sp}, L_{sc} and L_r are the total cycle inductances of the stators and rotor respectively; L_{mp} and L_{mc} are the mutual or magnetizing inductances.

The dynamic equations in (10-21) are usually represented in the selected d-q reference frame [6]. Fig. 5 shows the angle relationship of power machine stator, PW and CW rotors and CW stator to the selected reference frame.

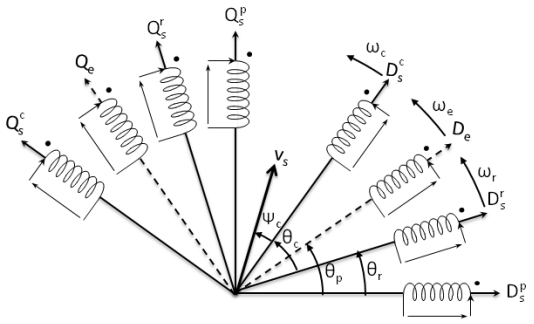

Fig. 5 Control winging reference D-Q frame

The general relationships between these quantities as well as the electrical speed of the rotor for the 50 Hz system are

$$\begin{cases} \omega_p = 2\pi \cdot 50 \\ \omega_r = \omega_p - \omega_r p_p \\ \omega_r = \omega_p - \omega_r (p_p + p_c) \end{cases} \quad (22)$$

The equation also shows the torque to be the function of the PW flux as well as the CW stator and rotor currents

$$C_{em} = \frac{3}{2}\left(p_p\left(\psi_{sp}^{d} i_{sp}^{q} - \psi_{sp}^{q} i_{sp}^{d}\right) + p_c L_{mc}\left(i_{sc}^{d} i_{r}^{q} - i_{sc}^{q} i_{r}^{d}\right)\right) \quad (23)$$

Finally, the mechanical model of BDFIG can be written as

$$J_g \frac{d\omega_m}{dt} = C_{em} - f_g \omega_m - C_L \quad (24)$$

Where ω_p and ω_c are the stators synchronous angular frequency; ω_r is the rotor's electrical angular speed; P_p and P_c are the number of poles of PW and CW respectively; C_{em} is the electromagnetic developed torque; C_L is the load torque; J_g is the rotor inertia; F_g is the rotor damping coefficient.

4. BDFIG CONTROLLER DESIGN

4.1. Control of the grid inverter

The various control strategies for the voltage source rectifier (VSR) have been proposed [5], [14] and will be briefly discussed here.

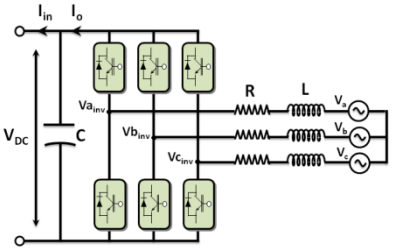

Fig. 6 VSR Circuit Model

The system can be written in a rotating reference frame by using Park transformation

$$\begin{bmatrix} v_q \\ v_d \end{bmatrix} = R \begin{bmatrix} i_q \\ i_d \end{bmatrix} + L \cdot s \begin{bmatrix} i_q \\ i_d \end{bmatrix} + \omega_e L \begin{bmatrix} i_q \\ -i_d \end{bmatrix} + \begin{bmatrix} v_{q_{inv}} \\ v_{d_{inv}} \end{bmatrix} \quad (25)$$

Where s is the derivation operation.

$$\begin{cases} P = \frac{3}{2}\left(v_d i_d + v_q i_q\right) \\ Q = \frac{3}{2}\left(v_q i_d + v_d i_q\right) \end{cases} \quad (26)$$

The voltage components in the Park frame V_{d_inv} and V_{q_inv} are given at the output of the PI regulator:

$$\begin{cases} v_d^* = -i_d(s\,L + R) + \left(\omega_e\,L\,i_q + v_d\right) \\ v_q^* = -i_q(s\,L + R) + \left(\omega_e\,L\,i_d\right) \end{cases} \quad (27)$$

In the Park reference frame, the voltage source components are $V_d = 0$ and $V_q = V_s$ and the powers can be written as

$$\begin{cases} P = \frac{3}{2} v_q i_q \\ Q = \frac{3}{2} v_q i_d \end{cases} \quad (28)$$

The complete block diagram of the VSR controller is shown in Fig.7.

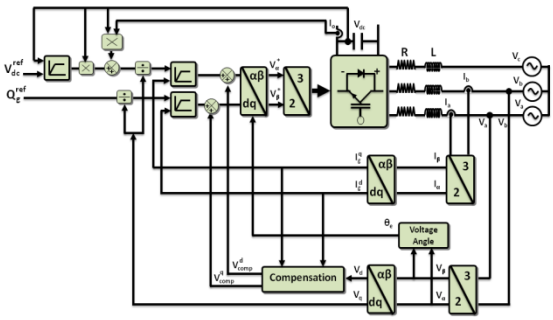

Fig. 7 Grid side VSR

4.2. Power winding side Controller

The developed control strategy is based on a loops control as shown in Fig. 8. Two regulation paths are implemented as in the classical vector control schemes: one control path regulates the d magnetizing currents and

the other one is dedicated to control the q active currents. In order to obtain a good decoupled control, the power machine flux orientation has been selected ($\psi_{sp}^{d} = |\psi_{sp}|$ and $\psi_{sp}^{q} = 0$). The obtained control strategy for the BDFIG is similar to the well-known stator field orientation control used in the DFIG. [6], [7], [14].

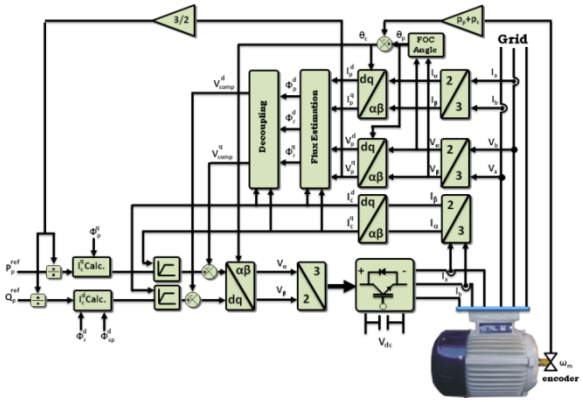

Fig. 8 Block diagram of BDFIG power control system

5. CONTROLLERS SYNTHESIS

5.1. PI controller synthesis

At present, the PI-type controller is most widely adopted in industrial application due to its simple structure, as shown Fig. 9. Its control signal is easily computed by combining proportional-integral terms

$$u(t) = \left[K_p + K_i\left(\frac{1}{s}\right)\right] e(t) \qquad (29)$$

The terms K_p and K_i represent respectively the proportional and integral gains.

The quotient B/A represents the transfer function to be controlled, where A and B are presently defined as follows:

$$A = R_{sc} + s\delta_3 \text{ and } B = 1 \qquad (30)$$

Where $\delta_3 = L_{sc} - \frac{L_{mc}^2 L_{sp}}{L_r L_{sp} - L_{mp}^2}$

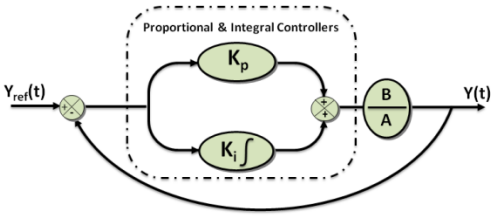

Fig. 9 System with PI controller

The controller terms can be calculated just specifying the natural frequency and damping of the close loop equivalent second order system. The desired natural frequency (ω_n) and damping (ξ) are set respectively to 37 rad/s and 70.7 %.

Allows determining the parameters of PI controller:

$$K_i = \omega_n^2 \cdot \delta_3 \qquad \text{and} \qquad K_p = 2 \cdot \xi \cdot \omega_n \cdot \delta_3 - R_{sc} \qquad (31)$$

The reason for the popular use of the PI-type controller is that this controller can be easily designed by adjusting only two controller parameters: K_p and K_i. In addition, its control performance can be accepted in many applications.

5.2. HFP+IC controller synthesis

In order to improve the performance PI control, we propose a HFP+IC controller, as shown in Fig. 10.

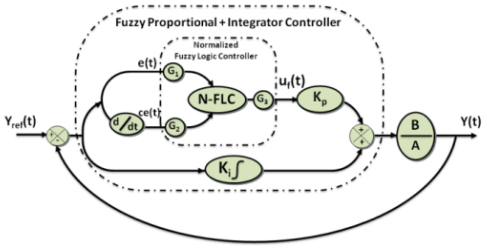

Fig. 10 HFP+IC controller scheme

This HFP+IC controller uses an fuzzy logic controller in place of the proportional term; while the integral term keeps unchanged

$$u(t) = \left[K_p u_f(t) + K_i\left(\frac{1}{s}\right)\right] e(t) \qquad (32)$$

Where K_i is identical to the conventional PI controller in Eq. (29), u_f (t) is the output of the fuzzy logic controller, and K_p is its proportional coefficient. The most important part in the HFP+IC controller is the FP term because it is responsible for improving overshoot and rise time. The conventional I term is mainly responsible for reducing a steady-state error if an actual value is close to a reference signal, [13,14-15].

The fuzzy logic controller is a standard one which has two inputs e(t) and ce(t) and an output $u_f(t)$. The membership functions used for the input and output fuzzy set are shown in Fig. 12. All the membership functions have asymmetrical shape with more crowding near the origin for higher precision at steady state [15-16].

The knowledge base involves defining the rules represented as IF-THEN rules statements governing the relationship between inputs and output variables in terms of membership functions [15-16]. In this stage the input variables e(t) and ce(t) are processed by the inference engine that executes 7×7 rules shown in rule Tab. 1.

After processing the inputs through knowledge base and inferencing mechanism the next stage is defuzzification. In this stage the fuzzy variables are converted into a crisp variable, [16]. This stage introduces different inference methods that can be used to produce the fuzzy set value for the output fuzzy variable u_f. In this, the center of gravity or centroid method is used to calculate the final fuzzy value u_f. The output function is given as:

$$u_f = \frac{\sum_{k=1}^{n} u_{f(k)} \cdot \mu(u_{f(k)})}{\sum_{k=1}^{n} \mu(u_{f(k)})} \qquad (33)$$

Where n is the total number of rules and $\mu(u_{f(k)})$ denotes the output membership value for k^{th} rule.

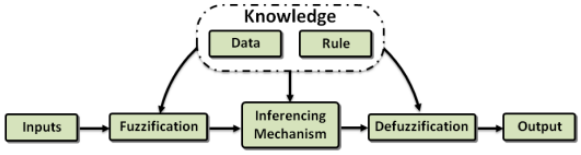

Fig. 11 Block diagram of fuzzy controller

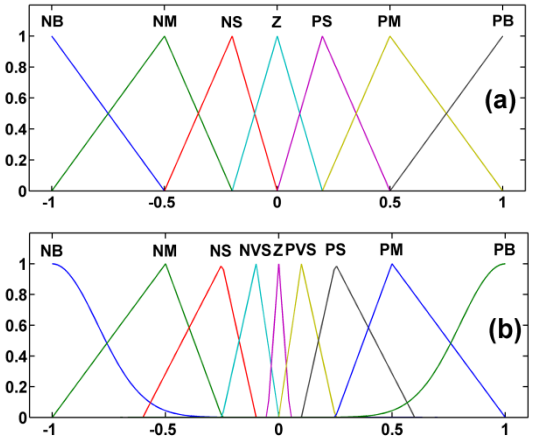

Fig. 12 Membership functions for: (a) error e and change of error ce and (b) output uf

6. SIMULATION RESULTS AND DISCUSSION

The aim of the control is to have measured active and reactive powers equal to the reference values. These powers must then be collected. In order to measure only the stator current of CW. The tow controllers have been tested using the indirect control method. The indirect control mode is based on the stator currents measurements of CW.

Table 1 Fuzzy rule base of the fuzzy logic controller

ce \ e	NB	NM	NS	Z	PS	PM	PB
NB	NB	NB	NB	NM	NS	NV	Z
NM	NB	NM	NM	NS	NV	Z	PV
NS	NB	NM	NS	NV	Z	PV	PS
Z	NM	NS	NV	Z	PV	PS	PM
PS	NS	NV	Z	PV	PS	PM	PB
PM	NV	Z	PV	PS	PM	PM	PB
PB	Z	PV	PS	PM	PB	PB	PB

6.1. Performances of the controller

The aim of this test is to analyze the influence of a speed variation of the BDFIG on active and reactive powers and d-q stator currents of CW. The speed varies from 75 rad/s (corresponds to 716.5 rpm) to 82.5 rad/s = 788 rpm. The results are shown in Fig. 13

.

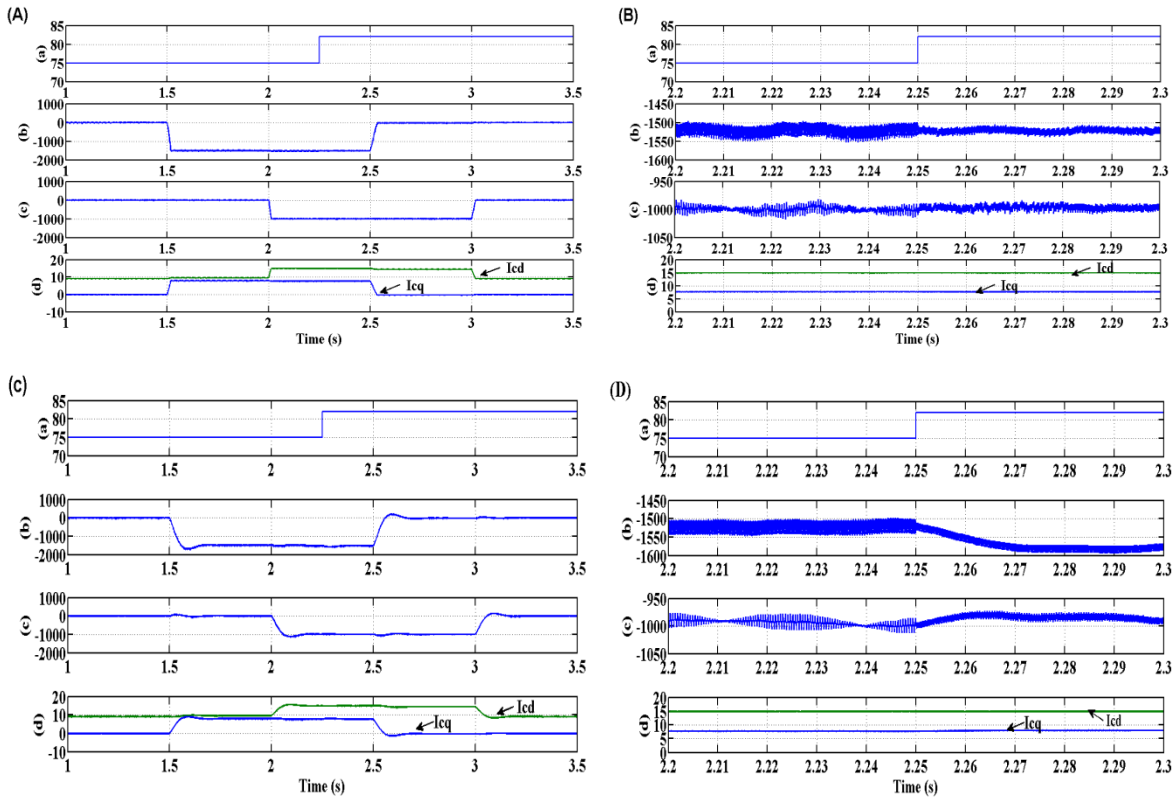

Fig. 13 Simulated results under various speed and stator reactive power steps. (A) hybrid fuzzy proportional plus integrator conventional controller. (B) Zoom of A. (C) PI Controller. (D) Zoom of C. (a) Rotor speed (rd/s). (b) Stator active power of PW (W). (c) Reactive power of PW (Var). (d) Direct and quadratic stator currents of CW (A)

The first test investigated to compare the both controllers is reference tracking by applying stator active and reactive power steps of PW, respectively. As shown in Fig. 13, the active power is stepped from 0 to -1.5 kW (export to grid) at 1.5 s and then backed to 0 at 2.5 s, the reactive power is stepped from 0 to -1 kW at 2 s and then backed to 0 at 3 s, while the machine's speed is maintained constant during the first change at 716.5 rad/s and at 788 rad/s during the second change. The results are presented in Fig. 13A and Fig. 13C.

This figure shows the limits of the PI controller which is only based on the machine's parameters and does not take into account any disturbances. Indeed, for this controller, a speed variation induces an important variation of the active and reactive powers (15% for active power and 5% for reactive power). The hybrid fuzzy proportional plus integrator conventional controller has a nearly perfect speed disturbance rejection, indeed; only very small power variations can be observed (less than 0.1% for active power and 2% for reactive power. This result is interesting for wind energy applications to ensure stability and quality of the generated power when the speed is varying.

6.2. Simulation of the whole system

The brushless doubly fed induction generator parameters used in the simulation are given as following.

Table 2 BDFIG Parameters used for Simulation

Turbine	
	Diameter = 4.6 m, Number of blades = 3, Hub height = 12 m, Gearbox = 18
BDFIG	
	2.5 Kw, 380 V, 50 Hz, 2 pole pairs, R_{sp} = 1.732 Ω, R_{sc} = 1.079 Ω, R_r = 0.473Ω, L_{sp} = 714.8 mH, L_{sc} = 121.7 mH, L_r = 132.6 mH.
Grid	
	U = 380 V, Z_{line} =R +jLω = 0.25 +j0.003.

The nominal dc link voltage was set at 410 V. The grid side converter behaves to keep the DC-link voltage constant, and it is controlled by a method similar to the dc voltage controller in a PWM voltage source rectifier [14].

The results of simulations are obtained for reactive power $Q_{ref} = 0$ and DC-link voltage E=410 V. Fig. 14 shows the wind speed. Fig. 15 presents the wind generator mechanical power. The decoupling effect of the between the direct and quadratic stator flux of PW is illustrated in Fig. 16. The stator currents and voltages waveforms of the BDFIG and the related expended plots are shown, respectively, in Fig. 17a, Fig. 17b, Fig. 17c and Fig. 17d (phase a). The PWM inverters are operated at 2 kHz; hence, the currents are almost sinusoidal. Fig. 18 gives the rotor current of the BDFIG. The grid voltage and current waveforms and these zoom are presented, correspondingly, in Fig. 19a and Fig. 19b. The stator active and reactive powers are plotted in Fig. 20. Fig. 21 shows the regulation of the DC-link voltage. It is maintained at a constant level (410 V) so that the real power extracted from the wind energy conversion system can pass through the grid.

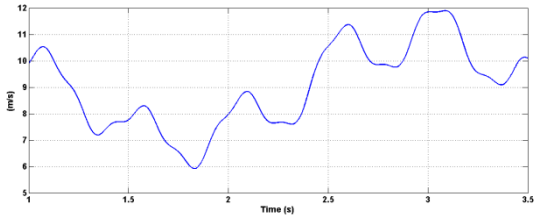

Fig. 14 Wind speed (V_w)

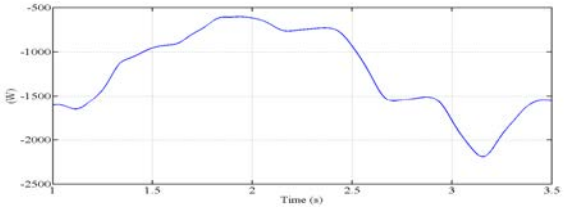

Fig. 15 Wind generator mechanical power (P_{mec})

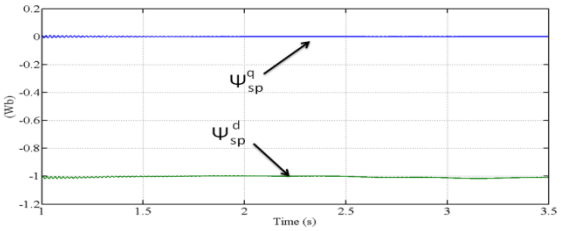

Fig. 16 Direct and quadratic stator flux of PW (ψ_{sp}^{q} and ψ_{sp}^{d})

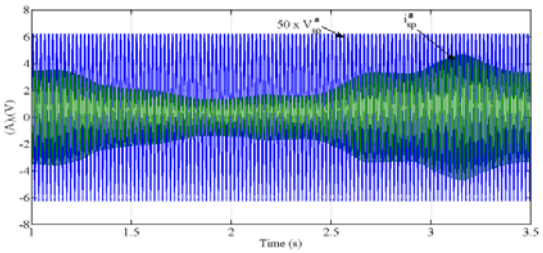

Fig. 17a Stator current and voltage of PW (I_{sp}^{a}, V_{sp}^{a})

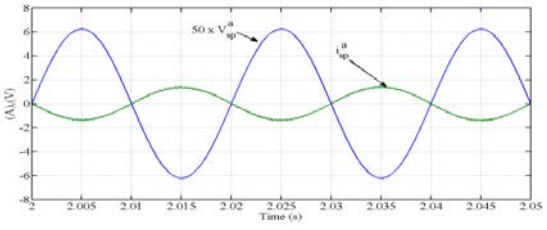

Fig. 17b Zoom of Stator current and voltage of PW (I_{sp}^{a}, V_{sp}^{a})

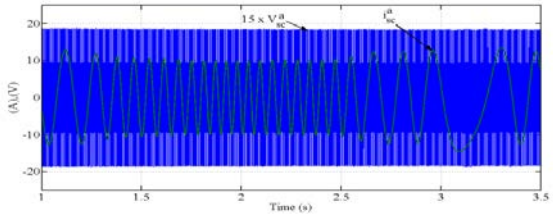

Fig. 17c Stator current and voltage of CW (I_{sc}^{a}, V_{sc}^{a})

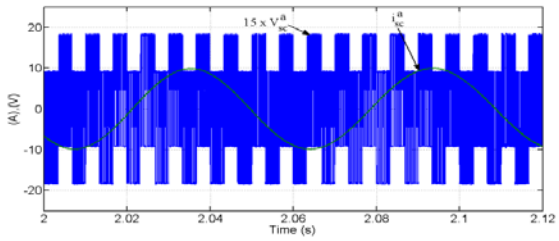

Fig. 17d Zoom of Stator current and voltage of CW (I_{sc}^{a}, V_{sc}^{a})

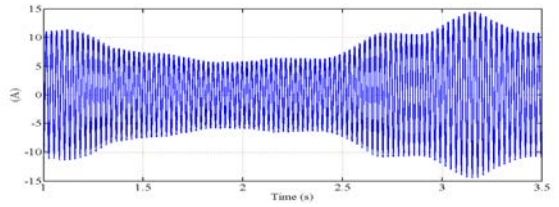

Fig. 18 Rotor current (I_{r}^{a})

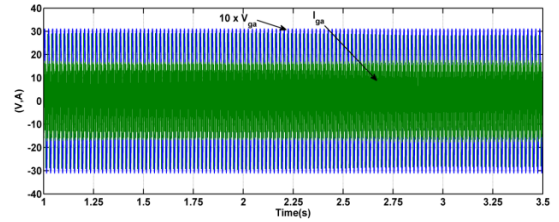

Fig. 19a Grid voltage and current (I_{g}^{a}, V_{g}^{a})

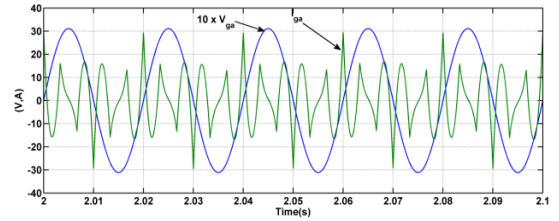

Fig. 19b Zoom of Grid voltage and current (I_{g}^{a}, V_{g}^{a})

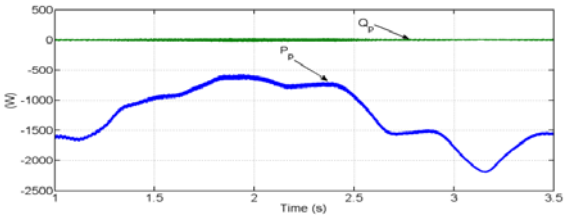

Fig. 20 Stator active and reactive powers(P_p, Q_p)

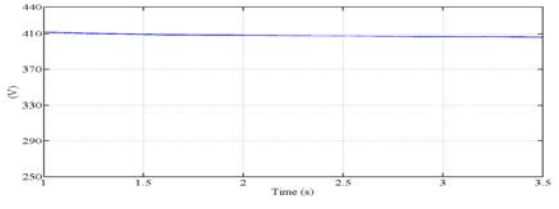

Fig. 21 DC-link voltage (E)

7. CONCLUSIONS

In this paper, we have presented a complete system to produce electrical energy with a BDFIG by the way of a wind turbine. The studied device is constituted of a BDFIG with the stator of PW directly connected to the grid and the stator of CW connected to the grid by the way of two converters (machine inverter and grid inverter). The control of the machine inverter has been presented first in order to regulate the active and reactive powers exchanged between the machine and the grid. Two different controllers are synthesized and compared. The performances of the two controllers are not similar. When the machine's speed is modified (which represents a perturbation for the system), the impact on the active and reactive powers values is important for PI where as it is almost non-existent for hybrid fuzzy proportional plus integrator conventional (HFP+IC).

The grid inverter has also been controlled with a PI controller in order to maintain the DC-bus voltage to a constant value. A test has been investigated with speed, active and reactive power variations showing negligible variations of the voltage.

The last part of the paper shows the simulation of the whole system behaviour with a turbine. The presented results show that intelligent control method as HFP+IC can be a very attractive solution for devices using BDFIG such as wind energy conversion systems. Indeed, most of the studied BDFIG control schemes use classical PI controllers but the comparison done in this paper show that the limits of this type of controller can have negative effects on the quality and the quantity of the generated power.

8. REFERENCES

[1] PROTSENKO, K. – DEWEI, Xu: "Modeling and control of brushless doubly fed induction generators in wind energy applications" IEEE Trans. Pow. Elec., Vol. 23, No.3, MAY 2008.

[2] AMIMEUR, H. – AOUZELLAGA, D. – ABDESSEMEDB, R. – GHEDAMSI, K.: Sliding mode control of a dual-stator induction generator for wind energy conversion systems, IJEP, Vol. 42, no. 1, pp. 60–70, Nov. 2012.

[3] POZA, J. – OYARBIDE, E. – SARASOLA, I. – RODRIGUEZ, M.: Unified reference frame dq model of the brushless doubly fed machine, IEE Proc. Electr. Power Appl., Vol. 153, No. 5, pp. 726-734, Sep. 2006.

[4] POZA, J. – OYARBIDE, E. – ROYE, D.: New vector control algorithm for brushless doubly fed machines, in Proceedings of IECON'02 Conference, Spain, Nov. 2002.

[5] PROTSENKO, K. – DEWEI, Xu: Modeling and control of brushless doubly fed induction generators in wind energy applications, APEC 2007.

[6] POZA, J. – OYARBIDE, E. – SARASOLA, I. – RODRIGUEZ, M.: "Vector control design and experimental evaluation for the brushless doubly fed machine", IET Electr. Power Appl, Vol. 3, Iss. 4,

2009, pp. 247–256.

[7] POITIERS, F. – BOUAOUICHE, T. – MACHMOUM, M.: Advanced control of a doubly-fed induction generator for wind energy conversion, Journal of EPSR, Vol.79, no 7, pp. 1085-1096, July 2009.

[8] WALLACE, A. K. – Spee, R. – Alexander, G. C.: The brushless doubly-fed machine: its advantages, applications and design methods in Proceedings of EM'06 Conference, 1993.

[9] SARASOLA, I. – POZA, J. – RODRIGUEZ, M. A. –ABAD, G.: Direct torque control design and experimental evaluation for the brushless doubly fed machine journal of ECM, Vol. 52, no. 2, pp. 1226-1234, Feb. 2011,

[10] SHIYI, S. – ABDI, E. – McMAHON, R.: Low-Cost Variable Speed Drive Based on a Brushless Doubly-fed Motor and a Fractional Unidirectional Converter, IEEE Trans. Industrial Electronics, Vol. 59, no. 1 pp. 317 – 325, 2012.

[11] RUNCOS, F. – CARLSON, R. – OLIVEIRA, A. – KUO-PEN, P. – SADOWSKI, N.: Performance Analysis of a Brushless Double Fed Cage Induction Generator, Proc. Nordic Wind Power Conference, 2004, pp. 1 – 8.

[12] SHIYI, S. – ABDI, E. – BARATI, F. – McMAHON, R.: Stator-Flux-Oriented Vector Control for Brushless Doubly Fed Induction Generator IEEE Trans. Industrial Electronics, Vol. 56, no. 10, pp. 4220 – 4228, 2009.

[13] WEI LI: Design of a hybrid fuzzy logic proportional plus conventional integral – derivative controller, IEEE Trans. Fuzzy system, vol. 6, No. 4, Nov. 1998.

[14] PENA, R. – CLARE, J. C. – ASHER, G. M.: Doubly fed induction generator using back-to-back PWM converters and its application to variable speed wind-energy generation, IEE Proc.-Electr. Power Appl., Vol. 143, No 3, May 1996.

[15] ZADEH, L. A.: Fuzzy Sets, Information and control, Vol. 8, pp. 338-353. 1965.

[16] SAHU, B. – MOHANTY, K. B. – PATI, S.: A Comparative Study on Fuzzy and PI Speed Controllers for Field-Oriented Induction Motor Drive, MEPS'10, pp. 7-14, 2010.

[17] YU, J. S. – KIM, S. H. – LEE, B. K. – WON, C. Y. – HUR, J.: Fuzzy-Logic-Based Vector Control Scheme for Permanent-Magnet Synchronous Motors in Elevator Drive Applications, IEEE Trans. Indus. elect., vol. 54, no. 4, august 2007.

Received April 27, 2013, accepted June 16, 2013

BIOGRAPHIES

Zoheir Tir was born on 16.04.1983 in Eloued, Algeria, received his undergraduate and Magister degrees in Electrical Engineering from Batna and Setif Universities in Algeria in 2007 and 2010, respectively. He is currently a D.Sc candidate at Batna University. He is member of the LEVRES research laboratory. His research project involves the modeling, simulation and control of electrical machines, particularly in the wind power generation.
Currently, he is a Teaching Assistant at the Faculty of Science and Technology, University of Eloued.

Rachid Abdessemed (Prof, PhD) was born in Batna, Algeria and got the MSc and PhD degrees in electrical engineering from Kiev Polytechnic Institute and Electrodynamic Research Institute Ukrainian Academy of Sciences in 1982. Currently, he is director of the LEB research laboratory. His research interests are the design and control of induction machines and converters, reliability, magnetic bearings and renewable energy.